



Published in final edited form as:

Nature. 2011 March 24; 471(7339): 513–517. doi:10.1038/nature09806.

The SETDB1 histone methyltransferase is recurrently amplified in and accelerates melanoma

Craig J. Ceol^{1,†,*}, Yariv Houvras^{1,2,*}, Judit Jane-Valbuena³, Steve Bilodeau⁴, David A. Orlando⁴, Valentine Battisti⁵, Lauriane Fritsch⁵, William M. Lin³, Travis J. Hollmann⁶, Fabrizio Ferré⁷, Caitlin Bourque¹, Christopher J. Burke¹, Laura Turner¹, Audrey Uong¹, Laura A. Johnson³, Rameen Beroukhim³, Craig H. Mermel³, Massimo Loda⁶, Slimane Ait-Si-Ali⁵, Levi A. Garraway³, Richard A. Young⁴, and Leonard I. Zon¹

¹Stem Cell Program and Hematology/Oncology, Children's Hospital Boston, Howard Hughes Medical Institute, Harvard Stem Cell Institute, Harvard Medical School, Boston, MA 02115, USA

² Massachusetts General Hospital Cancer Center, Harvard Medical School, Boston, MA 02114, USA

³ Departments of Medical Oncology, Cancer Biology, and Center for Cancer Genome Discovery, Dana-Farber Cancer Institute, Harvard Medical School, Boston, MA 02115, and The Broad Institute, Cambridge MA 02142, USA

⁴ Whitehead Institute for Biomedical Research, 9 Cambridge Center, Cambridge, MA 02142, USA

⁵ UMR7216 Epigénétique et Destin Cellulaire, CNRS, Université Paris-Diderot, 35 rue Hélène Brion, 75013 Paris, France

⁶ Center for Molecular Oncologic Pathology, Brigham and Women's Hospital, Dana-Farber Cancer Institute, Harvard Medical School, Boston, MA 02115, USA

⁷ A. Rossi Fanelli Biochemical Sciences Department, Sapienza University of Rome, Rome 00185, Italy

Users may view, print, copy, download and text and data- mine the content in such documents, for the purposes of academic research, subject always to the full Conditions of use: http://www.nature.com/authors/editorial_policies/license.html#terms

Correspondence and requests for materials should be addressed to L.I.Z. (zon@enders.tch.harvard.edu).

[†]Present address: Program in Molecular Medicine, Program in Cell Dynamics, and Department of Cancer Biology, University of Massachusetts Medical School, Worcester, MA 01605, USA

*These authors contributed equally to this work and are listed alphabetically.

Author contributions C.J.C., Y.H. and L.I.Z. conceived the project, designed and analyzed experiments, and wrote the manuscript. C.J.C. and Y.H. performed the zebrafish and contributed to the other experiments. J.J-V. performed tissue culture experiments. S.B. performed and analyzed ChIP-Seq experiments. V.B., L.F., S.A-S-A. performed SETDB1 biochemistry studies. L.A.J. performed fluorescence in situ hybridization studies. T.H. performed immunohistochemistry. W.M.L., R.B. and C.H.M. analyzed copy number data. D.A.O. analyzed WM451Lu SETDB1-overexpression microarray data. F.F. designed a database to manage and analyze tumor incidence data. C.B., C.B., L.T., and A.U., provided technical assistance. M.L., L.A.G., and R.A.Y. provided input in the preparation of the manuscript.

Author information The data discussed in this publication have been deposited in the National Center for Biotechnology Information Gene Expression Omnibus and are accessible through GEO Series GSE26372 (<http://www.ncbi.nlm.nih.gov/geo/query/acc.cgi?acc=GSE26372>). Reprints and permissions information is available at www.nature.com/reprints. L.I.Z. is a founder and stockholder of Fate, Inc. and a scientific advisor for Stemgent. Readers are welcome to comment on the online version of this article at www.nature.com/nature.

Supplementary Information is linked to the online version of the paper at www.nature.com/nature.

Abstract

The most common mutation in melanoma, *BRAF(V600E)*, activates the BRAF serine/threonine kinase and causes excessive MAPK pathway activity^{1,2}. *BRAF(V600E)* mutations are also present in benign melanocytic nevi³, highlighting the importance of additional genetic alterations in the genesis of malignant tumors. Such changes include recurrent copy number variations that result in the amplification of oncogenes^{4,5}. For certain amplifications, the large number of genes in the interval has precluded an understanding of cooperating oncogenic events. Here, we have used a zebrafish melanoma model to test genes in a recurrently amplified region on chromosome 1 for the ability to cooperate with *BRAF(V600E)* and accelerate melanoma. *SETDB1*, an enzyme that methylates histone H3 on lysine 9 (H3K9), was found to significantly accelerate melanoma formation in the zebrafish. Chromatin immunoprecipitation coupled with massively parallel DNA sequencing (ChIP-Seq) and gene expression analyses revealed target genes, including Hox genes, that are transcriptionally dysregulated in response to elevated *SETDB1*. Our studies establish *SETDB1* as an oncogene in melanoma and underscore the role of chromatin factors in regulating tumorigenesis.

To identify genes that promote melanoma we focused on genomic regions subject to copy number amplification in human tumor samples. In a study of 101 melanoma short-term cultures and cell lines, chromosome 1q21 (chr1: 147.2-149.2 Mb) was identified as a recurrently amplified interval (Fig. 1a)⁶. The same region was implicated in another comprehensive analysis of copy number variation in melanoma⁴. To functionally test candidate genes from this interval for the ability to accelerate melanoma we developed an assay in transgenic zebrafish in which *BRAF(V600E)* is overexpressed on a *p53* mutant background (Supplementary Fig. 1). Melanomas and melanocytes that develop in *Tg(mitfa:BRAF^{V600E}); p53(lf)* zebrafish⁷ are suppressed by a *mitfa(lf)* mutation. We engineered a transposon-based vector, miniCoopR, that rescues melanocytes and melanomas in a *Tg(mitfa:BRAF^{V600E}); p53(lf); mitfa(lf)* strain and drives expression of a candidate gene in these rescued tissues. We identified genes that were present in the 1q21 region and overexpressed as mRNAs based on Affymetrix microarrays. Candidate genes were cloned into the miniCoopR vector and injected into one-cell stage *Tg(mitfa:BRAF^{V600E}); p53(lf); mitfa(lf)* embryos. Tumor incidence curves of the resulting adults revealed that one gene in this interval, *SETDB1*, significantly accelerated melanoma onset ($p = 9.4 \times 10^{-7}$, logrank χ^2 ; Fig 1b,c and Supplementary Fig. 2). In addition to melanoma, *SETDB1* is focally amplified in non-small cell (NSCLC) and small cell lung cancer, ovarian cancer, hepatocellular cancer, and breast cancer (Supplementary Fig. 3). The anti-apoptotic gene *MCL1* resides near *SETDB1* in the 1q21 interval, and knockdown of *MCL1* was shown to diminish NSCLC proliferation and xenograft outgrowth⁸. However, *MCL1* is not overexpressed in the melanoma samples that were used to identify amplified genomic intervals, so it was not tested. No other gene accelerated melanomas, suggesting *SETDB1* is a critical gene amplified in the chromosome 1q21 interval. Using fluorescence in situ hybridization we observed *SETDB1* amplification in human melanoma short-term cultures (Supplementary Fig. 4), directly confirming the array-based copy number data from which our study originated.

Melanomas overexpressing *SETDB1* were more aggressive than control tumors when analyzed at an equivalent stage. The melanomas expressing *SETDB1* were more locally invasive than *EGFP* control tumors (Fig. 2a); 94% (*SETDB1*; n=18) vs. 53% (*EGFP*; n=17) of melanomas invaded into the muscle ($p=1.6\times 10^{-3}$, Fisher's exact) and 89% (*SETDB1*) vs. 35% (*EGFP*) invaded into the spinal column ($p=7.2\times 10^{-3}$, Fisher's exact). MiniCoopR-*SETDB1* melanomas had more extensive nuclear pleomorphism and larger nuclei as compared to control tumors (Supplementary Fig. 5). MiniCoopR-*SETDB1* tumors showed similar levels of BRAF protein as compared to control tumors, indicating that *SETDB1* did not accelerate melanoma formation by altering expression of the *BRAF(V600E)* transgene (Supplementary Fig. 6).

Melanocytes overexpressing *SETDB1* grew in confluent patches in zebrafish, unlike melanocytes in control zebrafish, which grew in a wild-type stripe pattern. We analyzed the genetic interactions that are responsible for these pigmentation differences. *SETDB1*-expressing melanocytes in the *Tg(mitfa:BRAF^{V600E}); mitfa(lf)* strain formed confluent patches, but *SETDB1*-expressing melanocytes in the *p53(lf); mitfa(lf)* strain grew in a striped pattern (Fig. 2b). Although *SETDB1* and *BRAF(V600E)* cooperated to override normal pigment patterning, no tumors arose in miniCoopR-*SETDB1* injected *Tg(mitfa:BRAF^{V600E}); mitfa(lf)* zebrafish, indicating *SETDB1* and *BRAF(V600E)* require loss of *p53* to form tumors.

Oncogenic *BRAF(V600E)* induces senescence in human nevi and in cultured mammalian melanocytes⁹, and we suspected that the pigmentation differences might result from a failure of senescence and excess melanocyte proliferation caused by *SETDB1*. Using senescence-associated β -Galactosidase (SA- β Gal) staining^{10,11}, we confirmed that *BRAF(V600E)* induces senescence of zebrafish melanocytes in vivo (Supplementary Fig. 7a,b,c). We stained miniCoopR-rescued melanocytes and found *SETDB1*-expressing melanocytes to be less senescent than those expressing *EGFP* (Fig. 2C). *SETDB1*-expressing melanocytes also lacked the flattened morphology of senescent cells (Supplementary Fig. 7d). These results suggest that *SETDB1* overexpression may contribute to melanoma formation by abrogating oncogene-induced senescence.

To understand the gene expression changes that occur when *SETDB1* is overexpressed, we performed microarray analyses of zebrafish melanomas. We defined a gene signature comprised of 69 human orthologs of genes downregulated in *SETDB1* overexpressing melanomas (Fig. 3a) and tested the relationship of this signature to *SETDB1* expression in human melanoma. Using gene set enrichment analysis (GSEA)^{12,13} we found that the gene signature was inversely correlated with *SETDB1* expression across a panel of 93 melanoma short-term cultures and cell lines (Fig. 3b). *SETDB1* overexpression leads to a broad pattern of transcriptional changes, including conserved downregulation of a group of genes enriched for Hox genes and transcriptional regulators.

To identify the direct targets of *SETDB1* genome-wide in melanoma, we performed chromatin immunoprecipitation followed by massively parallel sequencing (ChIP-Seq). We identified *SETDB1* targets from WM262, a melanoma short-term culture with high *SETDB1* expression, and WM451Lu, a melanoma short-term culture with low levels of

SETDB1 (Supplementary Fig. 8). These short-term cultures harbor the *BRAF(V600E)* mutation (Supplementary Fig. 9), and their proliferation is sensitive to changes in *SETDB1* levels (Supplementary Fig. 10, Supplementary Fig. 11). In murine embryonic stem cells (mESCs), SETDB1 binds to the promoters of developmental regulators, including HOX genes¹⁴. We observed differential binding of SETDB1 to genes in the HOXA cluster in melanoma cell lines with high vs. low SETDB1 expression; SETDB1 is bound to HOXA genes in WM262 cells, whereas there is minimal binding in WM451Lu cells (Fig. 3c, Supplementary Tables 1,2). SETDB1 catalyzes trimethylation of histone H3 lysine 9 (H3K9me3), thereby promoting repression of target genes. ChIP-Seq for the H3K9me3 mark showed that H3K9me3 is present at the HOXA locus in WM262 cells but absent in WM451Lu cells (Fig. 3c). HOX gene expression is inversely correlated with SETDB1 levels in melanoma short-term cultures (Fig. 3b), suggesting that enhanced target gene binding and repression may play a role in SETDB1-mediated melanoma acceleration. Additional ChIP-Seq, using WM262 cells, of the SETDB1 methyltransferase-stimulatory cofactor MCAF1/hAM¹⁵ suggests that the effects of SETDB1 overexpression are mediated in part by MCAF1/hAM (Supplementary Fig. 12).

We assayed effects of *SETDB1* overexpression on target genes by infecting WM451Lu cells with *SETDB1* lentivirus. Using SETDB1 ChIP-Seq data from WM451Lu, we determined that SETDB1-bound targets are significantly enriched in downregulated but not upregulated genes (Supplementary Fig. 13, Supplementary Table 3), suggesting that a major consequence of *SETDB1* amplification is repression of SETDB1-bound target genes. However, many SETDB1 target genes in both WM451Lu and WM262 lines are not methylated, and additional analyses show a relationship between higher *SETDB1* levels and elevated expression of many SETDB1 targets (Supplementary Fig. 14).

To obtain mechanistic insight into the role of SETDB1 in regulating gene expression, we undertook genetic and biochemical studies that evaluate methyltransferase activity. Recently, a complex containing SETDB1 and the H3K9 methyltransferases SUV39H1, G9a and GLP was discovered¹⁶. To examine the possibility that other methyltransferases act with *SETDB1* to modulate melanoma onset, we tested whether *SUV39H1* could accelerate melanoma formation in zebrafish. As with *SETDB1*, overexpression of *SUV39H1* led to the formation of confluent melanocyte patches and accelerated melanoma onset (Fig. 3d). We next examined the consequences of mutations that render SETDB1 enzymatically inactive. Enzymatically-deficient SETDB1 was capable of incorporating into the methyltransferase complex in vitro (Fig. 3e) and in vivo (Supplementary Fig. 15). Furthermore, in the context of enzymatically-deficient SETDB1, the complex retained methyltransferase activity (Fig. 3f, Supplementary Fig. 16) and binding site localization (Supplementary Fig. 17). Lastly, melanoma incidence curves from two methyltransferase-deficient SETDB1 mutants were similar to each other and to wild-type SETDB1 (Fig. 3d). Our studies suggest a model in which activity of the methyltransferase complex containing SETDB1 and SUV39H1 causes alterations of gene expression that lead to melanoma acceleration.

To determine the extent of SETDB1 overexpression in human melanomas, and to examine potential clinical implications, we performed immunohistochemistry (IHC) on melanoma tissue microarrays. After confirming antibody specificity (Supplementary Fig. 18), we

observed high levels of SETDB1 expression in 5% of normal melanocytes (n=20), 15% of benign nevi (n=20), and 70% of malignant melanoma (n=91; Fig. 4). Based on our observations of premalignant melanocytic lesions in zebrafish, we speculate that human nevi harboring SETDB1 overexpression may have a higher likelihood of oncogenic progression as compared with nevi that show basal levels of expression. These data indicate that the majority of malignant melanomas demonstrate overexpression of SETDB1 protein.

In this study we adapted the zebrafish as a platform for cancer gene discovery. Through the creation and analysis of over 3000 transgenic animals, *SETDB1* was identified as a gene capable of accelerating melanoma formation in cooperation with *BRAF(V600E)*. Amplification of 1q21 in melanoma does not preferentially co-occur with the *BRAF(V600E)* mutation (p=0.28, 2 sample t-test). Therefore, it is likely that the tumor-promoting activity of *SETDB1* is not exclusively dependent on *BRAF(V600E)*, which is common in melanomas but found less frequently in other tumor types with 1q21 amplification. SETDB1 forms a multimeric complex with SUV39H1 and other H3K9 methyltransferases. Based on our findings we speculate that *SETDB1* overexpression can increase activity of the H3K9 methyltransferase complex, leading to alterations in target specificity. Inactivating mutations in both histone methyltransferases and demethylases were recently described in renal cell carcinoma^{17,18}. Our study lends functional support to the notion that perturbation of histone methylation promotes cancer. *SETDB1* is focally amplified in a broad range of malignancies, suggesting that alterations in histone methyltransferase activity could define a biologically related subset of cancers.

Methods Summary

miniCoopR Assay

miniCoopR was constructed by inserting a zebrafish *mitfa* minigene (promoter + open reading frame + 3'UTR) into the BglIII site of pDestTol2pA2¹⁹. Individual MiniCoopR clones were created by Gateway multisite recombination using human, full-length open reading frames (Invitrogen). 25pg of each MiniCoopR-Candidate clone and 25pg of *tol2* transposase mRNA were microinjected into one-cell embryos generated from an incross of *Tg(mitfa:BRAF^{V600E}); p53(lf); mitfa(lf)* zebrafish. Rescued animals were scored weekly for the presence of visible tumor.

Senescence Assay

SA-βGal staining was performed as described¹⁰, except that scales plucked from the dorsum of melanocyte-rescued zebrafish were stained instead of tissue sections. This assay was performed in an *albino(b4)* mutant background so melanin pigment would not obscure βGal staining. Experimental animals were injected with 20pg miniCoopR-*SETDB1* + 10pg miniCoopR-*EGFP* and controls with 30pg miniCoopR-*EGFP*. Rescued melanocytes were recognized as EGFP-positive cells.

Gene Expression

From zebrafish, total RNA was extracted from four miniCoopR-*SETDB1* melanomas and four miniCoopR-*EGFP* melanomas. Total RNA from each was used for synthesis of cDNA,

which was hybridized to a Nimblegen 385K array (catalog 071105_Zv7_EXPR). Zebrafish genes downregulated by *SETDB1* were selected by fold change (*EGFP/SETDB1*) > 5 and filtered by a 'SETDB1 specificity score', which was defined as a fold change of >3 when comparing *Tg(mitfa:BRAF^{V600E}); p53(lf)* melanomas to miniCoopR-*SETDB1* melanomas.

Immunohistochemistry

Human melanoma tissue microarrays (TMAs) were analyzed by immunohistochemistry for SETDB1 using rabbit polyclonal Ab (Sigma HPA018142, 1:200) and a mouse monoclonal Ab 4A3 (Sigma, WH0009869M7, 1:400) with a purple substrate for the secondary antibody (Vector Labs, VIP Substrate). A methyl green counterstain was used.

Supplementary Material

Refer to Web version on PubMed Central for supplementary material.

Acknowledgements

We thank David Harrington, Richard White and Yi Zhou for helpful discussions, Christian Lawrence, Isaac Adatto and Li-Kun Zhang for expert fish care, Garrett Frampton for bioinformatics assistance, and Kristen Kwan, Chi-Bin Chien, and Jesse Boehm for reagents. This work was supported by grants from the Damon Runyon Cancer Research Foundation (C.J.C – DRG-1855-05), Charles A. King Trust Foundation (C.J.C.), a Young Investigator Award from the American Society of Clinical Oncology (Y.H.), Canadian Institutes of Health Research (S.B.) and National Institutes of Health (C.J.C. – K99AR056899-02; Y.H. – K08DK075432-04; R.A.Y. – CA146455, HG002668; L.I.Z. – DK53298-08).

References

1. Davies H, et al. Mutations of the BRAF gene in human cancer. *Nature*. 2002; 417(6892):949–954. [PubMed: 12068308]
2. Wan PT, et al. Mechanism of activation of the RAF-ERK signaling pathway by oncogenic mutations of B-RAF. *Cell*. 2004; 116(6):855–867. [PubMed: 15035987]
3. Pollock PM, et al. High frequency of BRAF mutations in nevi. *Nat Genet*. 2003; 33(1):19–20. [PubMed: 12447372]
4. Curtin JA, et al. Distinct sets of genetic alterations in melanoma. *N Engl J Med*. 2005; 353(20): 2135–2147. [PubMed: 16291983]
5. Garraway LA, et al. Integrative genomic analyses identify MITF as a lineage survival oncogene amplified in malignant melanoma. *Nature*. 2005; 436(7047):117–122. [PubMed: 16001072]
6. Lin WM, et al. Modeling genomic diversity and tumor dependency in malignant melanoma. *Cancer Res*. 2008; 68(3):664–673. [PubMed: 18245465]
7. Patton EE, et al. BRAF mutations are sufficient to promote nevi formation and cooperate with p53 in the genesis of melanoma. *Curr Biol*. 2005; 15(3):249–254. [PubMed: 15694309]
8. Beroukhi R, et al. The landscape of somatic copy-number alteration across human cancers. *Nature*. 2010; 463(7283):899–905. [PubMed: 20164920]
9. Michaloglou C, et al. BRAFE600-associated senescence-like cell cycle arrest of human naevi. *Nature*. 2005; 436(7051):720–724. [PubMed: 16079850]
10. Dimri GP, et al. A biomarker that identifies senescent human cells in culture and in aging skin in vivo. *Proc Natl Acad Sci U S A*. 1995; 92(20):9363–9367. [PubMed: 7568133]
11. Santoriello C, et al. Expression of H-RASV12 in a zebrafish model of Costello syndrome causes cellular senescence in adult proliferating cells. *Dis Model Mech*. 2009; 2(1-2):56–67. [PubMed: 19132118]

12. Subramanian A, et al. Gene set enrichment analysis: a knowledge-based approach for interpreting genome-wide expression profiles. *Proc Natl Acad Sci U S A*. 2005; 102(43):15545–15550. [PubMed: 16199517]
13. Mootha VK, et al. PGC-1alpha-responsive genes involved in oxidative phosphorylation are coordinately downregulated in human diabetes. *Nat Genet*. 2003; 34(3):267–273. [PubMed: 12808457]
14. Bilodeau S, Kagey MH, Frampton GM, Rahl PB, Young RA. SetDB1 contributes to repression of genes encoding developmental regulators and maintenance of ES cell state. *Genes Dev*. 2009; 23(21):2484–2489. [PubMed: 19884255]
15. Wang H, et al. mAM facilitates conversion by ESET of dimethyl to trimethyl lysine 9 of histone H3 to cause transcriptional repression. *Mol Cell*. 2003; 12(2):475–487. [PubMed: 14536086]
16. Fritsch L, et al. A subset of the histone H3 lysine 9 methyltransferases Suv39h1, G9a, GLP, and SETDB1 participate in a multimeric complex. *Mol Cell*. 2010; 37(1):46–56. [PubMed: 20129054]
17. Dalgliesh GL, et al. Systematic sequencing of renal carcinoma reveals inactivation of histone modifying genes. *Nature*. 2010; 463(7279):360–363. [PubMed: 20054297]
18. van Haaften G, et al. Somatic mutations of the histone H3K27 demethylase gene UTX in human cancer. *Nat Genet*. 2009; 41(5):521–523. [PubMed: 19330029]
19. Kwan KM, et al. The Tol2kit: a multisite gateway-based construction kit for Tol2 transposon transgenesis constructs. *Dev Dyn*. 2007; 236(11):3088–3099. [PubMed: 17937395]
20. Beroukhi R, et al. Assessing the significance of chromosomal aberrations in cancer: methodology and application to glioma. *Proc Natl Acad Sci U S A*. 2007; 104(50):20007–20012. [PubMed: 18077431]
21. Nisolle M, et al. Immunohistochemical study of the proliferation index, oestrogen receptors and progesterone receptors A and B in leiomyomata and normal myometrium during the menstrual cycle and under gonadotrophinreleasing hormone agonist therapy. *Hum Reprod*. 1999; 14(11): 2844–2850. [PubMed: 10548634]

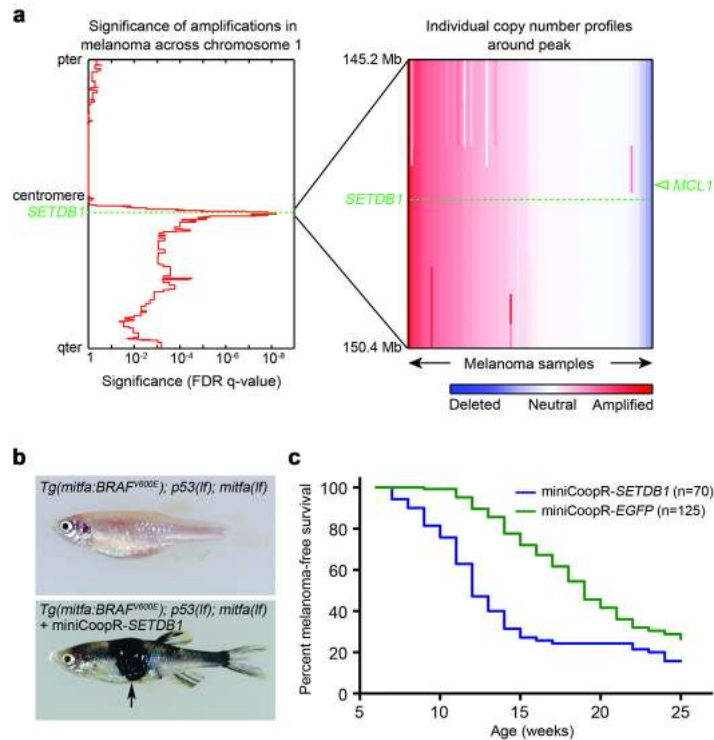


Figure 1. *SETDB1* accelerates melanoma formation in zebrafish

a, Left, significance of copy number amplification in human melanoma samples determined using genomic identification of significant targets in cancer (GISTIC)^{8,20}. q-values (x-axis) are plotted across chromosome 1. Right, copy number profiles of the 1q21 interval in melanoma samples. The positions of *SETDB1* (dotted line) and *MCL1* (arrowhead) are indicated. **b**, The *Tg(mitfa:BRAF^{V600E}); p53(lf); mitfa(lf)* strain (top) injected with miniCoopR-cloned candidate oncogenes. Animals injected with miniCoopR-*SETDB1* (bottom) have rescued melanocytes and rapidly develop melanomas (arrow). **c**, Melanoma-free survival curve of miniCoopR-*SETDB1* (weighted average of 2 independent experiments, n=70) and miniCoopR-*EGFP* (weighted average of 3 independent experiments, n=125) injected zebrafish.

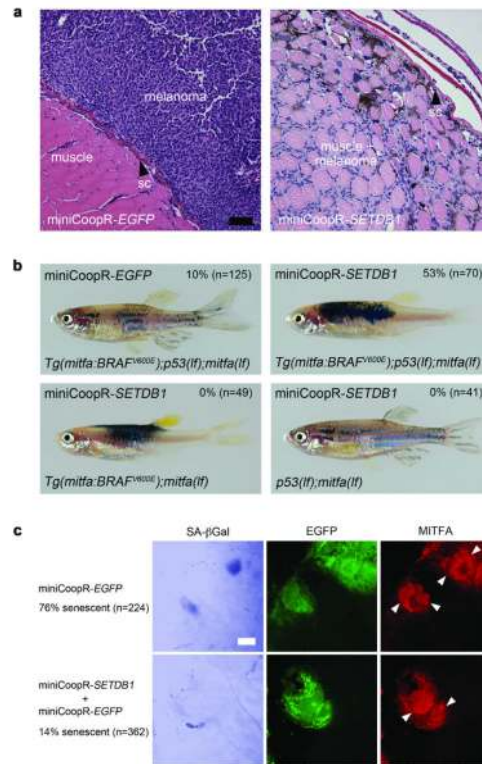


Figure 2. *SETDB1* effects on melanoma cells and melanocytes

a, Hematoxylin and eosin-stained transverse sections of zebrafish melanomas at two weeks post onset. At this time point dorsal miniCoopR-*EGFP* melanomas (left) display exophytic growth, whereas miniCoopR-*SETDB1* melanomas (right) have invaded from the skin, through the collagen-rich stratum compactum of the dermis (sc), into the underlying musculature. Scale bar = 70 μ m. **b**, *SETDB1* interacts with *BRAF(V600E)* to affect pigmentation pattern, but a *p53(lf)* mutation is required to form melanomas. MiniCoopR-*EGFP* or MiniCoopR-*SETDB1* was injected into the indicated transgenic strains. Percentages indicate melanoma incidence at 12 weeks of age. **c**, *SETDB1* abrogates *BRAF(V600E)*-induced senescence. Left, brightfield pseudocolored photomicrographs of SA- β Gal staining performed on scale-associated melanocytes. Middle and right, fluorescent photomicrographs of the same melanocytes. miniCoopR-rescued melanocytes in this experiment express *mitfa* promoter-driven EGFP (middle) and the MITFA protein (right). Multiple nuclei (arrowheads) are present in *BRAF(V600E)*-expressing melanocytes. Percentage of senescent melanocytes is indicated at left ($p = 7.3 \times 10^{-51}$, χ^2). Scale bar = 10 μ m.

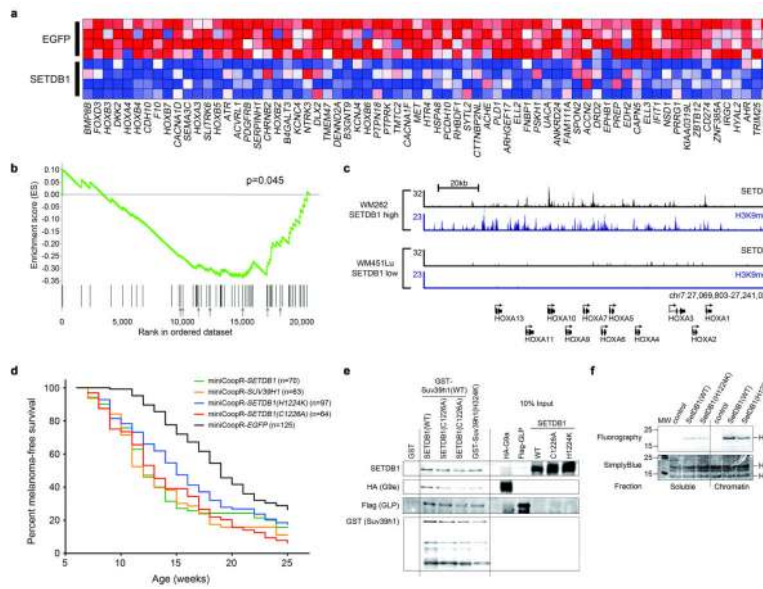


Figure 3. SETDB1 target gene regulation and HMTase complex formation

a, Heat map of genes downregulated in zebrafish melanomas that overexpress *SETDB1* compared with control (*EGFP*) melanomas. **b**, Graphical representation of the rank-ordered gene list derived from a panel of human melanoma short-term cultures stratified based on *SETDB1* expression level. GSEA shows that homologs of zebrafish *SETDB1*-downregulated genes are similarly downregulated in human melanomas as levels of *SETDB1* increase (ES = -0.35, NES = -1.43, FDR *q*-val = 0.045, *p* = 0.045). Arrows indicate positions of HOX genes. **c**, *SETDB1* and H3K9me3 ChIP-Seq profiles at the HOXA locus in human melanoma cells. The number of sequence reads is shown on the y axis. **d**, Melanoma-free survival curves of zebrafish expressing *SUV39H1* ($p = 6.74 \times 10^{-8}$ vs. *miniCoopR-EGFP*, logrank ⁷²) and the methyltransferase-deficient *SETDB1(H1224K)* ($p = 0.24$ vs. *miniCoopR-SETDB1*, $p = 8.4 \times 10^{-5}$ vs. *miniCoopR-EGFP*) and *SETDB1(C1226A)* ($p = 0.20$ vs. *miniCoopR-SETDB1*, $p = 1.3 \times 10^{-11}$ vs. *miniCoopR-EGFP*) variants. **e**, In vitro reconstitution of methyltransferase complexes. Sequential purification of GST-tagged SUV39H1, Flag-tagged GLP and HA-tagged G9a proteins was followed by western blotting using antibodies shown on left. **f**, Histone methylation assays on complexes purified from C2C12 cells.

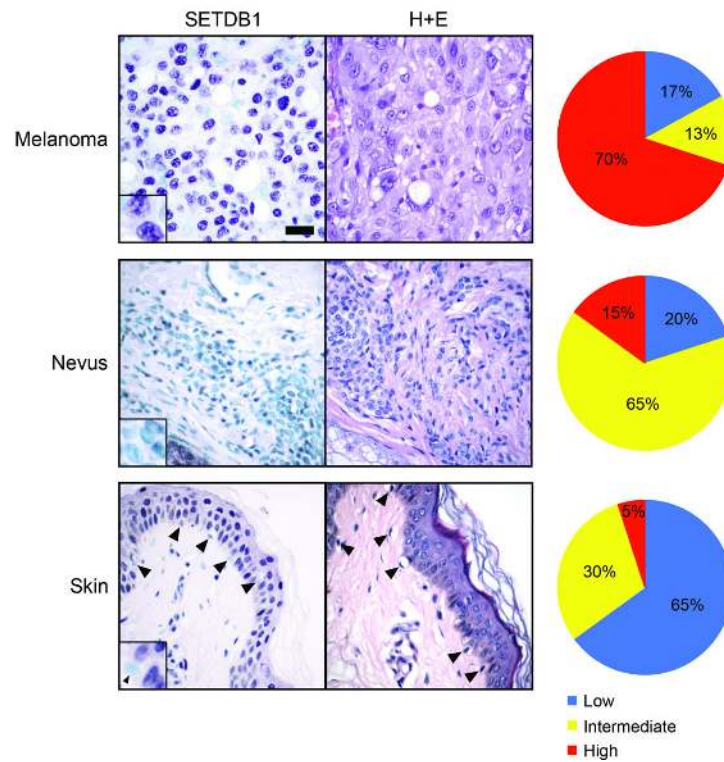


Figure 4. High expression of SETDB1 protein is common in human melanomas but not nevi or normal melanocytes

Immunohistochemical staining of SETDB1 (left) and hematoxylin and eosin (H+E) staining (center). SETDB1 expression (right) was scored on malignant melanoma (top; n=91), nevi (middle; n=20) and normal skin (bottom; n=20). SETDB1 expression was measured as described in Methods. Summarized and raw data from two independent antibodies are described in Supplementary Tables 4 and 5, respectively. Scale bar = 30 μ m, insets are 2.5x magnified.